Laser light scattering studies of soluble high performance fluorine-containing polyimides, 1

Polyimide synthesized from 2,2′-bis(3,4-dicarboxyphenyl)-hexafluoropropane dianhydride and 2,2′-(trifluoromethyl)-4,4′-biphenyldiamine

*Simon Chi Man Kwan, Chi Wu**

Department of Chemistry, The Chinese University of Hong Kong, Shatin, N.T., Hong Kong

Fuming Li, Edward P. Savitski, Frank W. Harris, Stephen Z. D. Cheng

Maurice Morton Institute of Polymer Science, Department of Polymer Science, The University of Akron, OH, 44325-3909, USA

(Received: November 1, 1996; revised manuscript of February 21, 1997)

SUMMARY:

Five fractions of a polyimide synthesized from 2,2′-bis(3,4-dicarboxyphenyl)hexafluoropropane dianhydride (6FDA) and 2,2′-(trifluoromethyl)-4,4′-biphenyldiamine (PFMB) (6FDA/PFMB) in tetrahydrofuran (THF) at 30 °C were investigated by a combination of static and dynamic laser light scattering (LLS). The relations of $\langle R_h \rangle$ (nm) = $2.38 \times 10^{-2} \bar{M}_w^{0.560}$ and A_2 (mol · cm^{-3} · g^{-2}) = $2.1 \times 10^{-1} \bar{M}_w^{-0.43}$ were established, where $\bar{M}_w$, $\langle R_h \rangle$ and A_2 are weight-average molecular weight, average hydrodynamic radius and second virial coefficient, respectively. A combination of $\bar{M}_w$ and the translational diffusion coefficient distribution $G(D)$ leads to a relation of D(cm^2/s) = $2.41 \times 10^{-4} M^{-0.564}$. With this relation, we successfully convert each $G(D)$ into a corresponding molecular weight distribution (MWD). On the basis of the Benoit-Doty theory, we found that the persistence length and the Flory characteristic ratio C_∞ of the 6FDA-PFMB chain are ~3.3 nm and ~40, respectively, indicating that the 6FDA-PFMB chain is more extended than typical random-coil chains. On the other hand, the ratio of the radius of gyration to the hydrodynamic radius, i.e., $\langle R_g \rangle / \langle R_h \rangle \sim 1.8$, together with the values of the exponents (~0.56) indicate that the 6FDA-PFMB chain has a coil chain conformation. Therefore, the 6FDA-PFMB chain has an extended coil conformation in THF at 30 °C.

Introduction

Aromatic polyimides are a kind of high performance polymers with high thermal and chemical stability, good solvent resistance and excellent electrical and mechanical properties[1]. They have been widely used in industry as the optical coating, adhesives, dielectric insulators, etc. The study of their molecular parameters are constantly required in their developments and applications. However, due to the high contents of aromatic rings, it is normally difficult to dissolve polyimides in common organic solvents, so that the study of their solution properties, such as the polymer

 CCC 1022-1352/97/$10.00

chain conformation, has been hindered[2]. In the past, the solution properties and molecular parameters of these insoluble polyimides have to be estimated from their precursor, e.g., poly(amic acid) formed in the first-stage reaction of an aromatic diamine with an anhydride, which leads to several serious problems[3–4], such as the unusual polyelectrolyte effects in the precursor solutions and a large difference between the chain dimensions of precursor and polymer. It is obvious that the development of a high-quality polyimide requires a direct measurement of physical properties of polyimides in solution.

Recently, soluble high performance polyimides have been developed[2]. One of the method is to fluorinate a given monomer so that aromatic rings are twisted and the interaction between the polymer chains are suppressed. Moreover, after introducing these fluorinated groups, the refractive index, water absorption and dielectric constant of these fluorinated polyimides are significantly reduced, which greatly enhance their electric properties[5,6].

In this study, the soluble polyimide poly[2,2′-bis(3,4-dicarboxyphenyl)hexafluoropropanedianhydride/2,2′-(trifluoromethyl)-4,4′-biphenyldiamine] (6FDA-PFMB) was synthesized via a one-step polycondensation[7,8]. In comparison with a two-step reaction, this one-step reaction has two advantages: a higher molecular weight and a narrower polydispersity. The structure of 6FDA-PFMB is as follows:

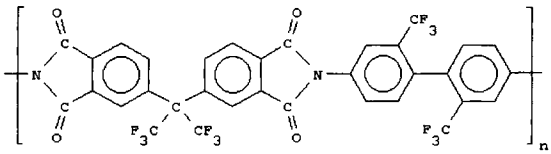

The backbone of this polyimide contains one flexible hexafluoropropane linkage and two trifluoromethyl groups on the aromatic rings. As mentioned before, the introduction of these fluorinated groups leads to its high performance physical and mechanical properties and solubility in common organic solvents, such as tetrahydrofuran (THF) and methyl ethyl ketone (MEK), which makes a direct study of its solution properties possible.

Experimental part

Sample preparation

The synthesis of 6FDA-PFMB has been detailed earlier[7,8]. Five fractions of a crude 6FDA-PFMB sample were collected using of a Waters Fraction Collector in conjunction with a Waters 150 CV chromatography system consisted of a series of four Waters Ultrastyragel columns in the order of 10^5, 10^4, 10^3, and 10^2 nm, wherein ACS regent grade tetrahydrofuran THF was used as the mobile phase and the flow rate was 1.0 mL/min. The collected fractions were transferred into pretared flasks to evaporate the solvent and were dried in vacuum for 24 h at 125 °C prior to the experiments. These fractions are termed 6FDA-1, 6FDA-2, 6FDA-3, 6FDA-4 and 6FDA-5 hereinafter. Analytical reagent grade THF as solvent was dried by sodium and then distilled under nitrogen before use.

All polymer solutions were clarified at room temperature using 0.1-μm or 0.2-μm inorganic membrane filter (Whatman) depending on the polymer molecular weight.

Laser light scattering (LLS)

A modified commercial light-scattering spectrometer (ALV/SP-125) equipped with an ALV-5000 multi-τ digital time correlator and solid state laser (ADLAS DPY 425II, output power ≈400 mW at $\lambda_0 = 532$ nm) was used as the light source. The primary beam is vertically polarized with respect to the scattering plane. In static LLS, the instrument was calibrated using toluene to make sure that the fluctuation of the scattering intensity from toluene after the angular correction is less than ±2% in a wide angular range of 6° – 154°. The detail of the LLS instrumentation and theory can be found elsewhere[9,10]. All LLS measurements were carried out at 30.0 ± 0.1 °C. In static LLS, the angular dependence of the excess absolute time-averaged scattered intensity, known as the excess Rayleigh ratio, $R_{vv}(q)$, was measured. For a dilute polymer solution measured at a low scattering angle, $R_{vv}(q)$ can be related to the weight-average molecular weight, $\bar{M}_w$, the second virial coefficient, A_2, and root mean square z-average radius of gyration, $\langle R_g^2 \rangle_z^{1/2}$ (or simply written as $\langle R_g \rangle$), as[11]

$$\frac{KC}{R_{vv}(q)} \approx \frac{1}{\bar{M}_w}\left(1 + \frac{1}{3}\langle R_g^2 \rangle_z q^2\right) + 2A_2C \tag{1}$$

where $K = 4\pi^2 n^2 (dn/dC)^2/(N_A \lambda_0^4)$ and $q = (4\pi n/\lambda_0)\sin(\theta/2)$ with N_A, dn/dC, n and λ_0 being Avogadro number, the specific refractive index increment, the solvent refractive index and the wavelength of light in vacuo, respectively. Measuring $R_{vv}(q)$ at a set of C and q, we are able to determine $\bar{M}_w$, $\langle R_g \rangle$, and A_2 from a Zimm plot which incorporate the extrapolation of $q \rightarrow 0$ and $C \rightarrow 0$ on a single grid.

In dynamic LLS, a precise intensity-intensity time correlation function $G^{(2)}(t, q)$ in the self-beating mode was measured and $G^{(2)}(t, q)$ is related to the normalized first-order electric field time correlation function, $g^{(1)}(t, q)$ as[10]

$$G^{(2)}(t,q) = \langle I(t,q)I(0,q)\rangle = A[1 + \beta|g^{(1)}(t,q)|^2] \tag{2}$$

where A is a measured base line; β, a parameter depending on the coherence of the detection; and t, the delay time. It should be stated that in this study A is not an adjustable parameter. Instead, we insisted on the agreement between A and the calculated baseline within 0.1% in all dynamic LLS experiments. This requires a very careful solution preparation (i.e., dust free).

Results and discussion

Fig. 1 shows a typical plot of the refractive index increment (Δn) versus concentration (C) for 6FDA-PFMB in THF at 30 °C. The line represents a least-square fitting, which leads to a specific refractive index increment of $dn/dC = 0.182 \pm 0.001$ mL/g at $T = 30.0$ °C and $\lambda_0 = 532$ nm. Eq. 1 shows that both $\bar{M}_w$ and A_2 depend on $(dn/dC)^2$, so that the accurate dn/dC value obtained in Fig. 1 has ensured a good characterization of $\bar{M}_w$ and A_2. It is worth noting that Δn was measured using a recently developed novel refractometer which is incorporated into our LLS spectrometer, wherein the same laser light source is used in both LLS and the refractometer,

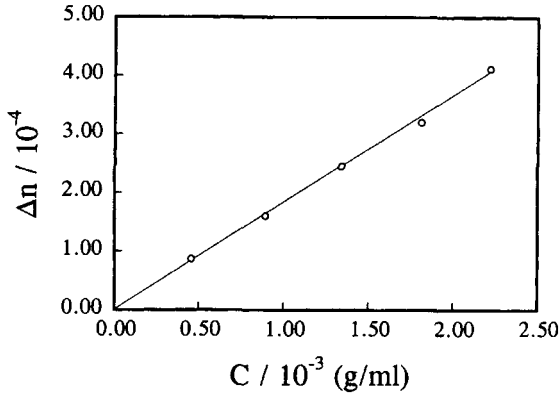

Fig. 1. Typical plot of the refractive index increment (Δn) versus concentration (C) for 6FDA-PFMB in THF at $T = 30\,^{\circ}C$ and $\lambda = 532$ nm

so that there is no wavelength correction for dn/dC. The detail of refractometer can be found elsewhere[12].

Fig. 2 shows a typical Zimm plot for 6FDA-PFMB in THF at 30 °C, where C ranges from 2×10^{-4} to 1×10^{-3} g/mL. From each Zimm plot, we were able to determine the values of $\bar{M}_w$, $\langle R_g \rangle$ and A_2 from $[KC/R_{vv}(q)]_{c\to 0,\theta\to 0}$, $[KC/R_{vv}(q)]_{c\to 0}$,

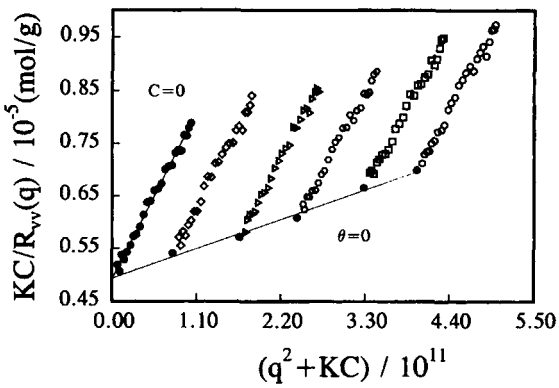

Fig. 2. Typical Zimm-plot of 6FDA-PFMB in THF at $T = 30\,^{\circ}C$, where C ranges from 2×10^{-4} to 1×10^{-3} g/mL

versus q^2 and $[KC/R_{vv}(q)]_{\theta\to 0}$ versus C, respectively. The static LLS results are summarized in Tab. 1. The positive A_2 values indicate that THF is a good solvent for 6FDA-PFMB at 30 °C. As expected, A_2 decreases as $\bar{M}_w$ increases except for the case of 6FDA-3. The 6FDA-4 and 6FDA-5 chains are so short that $R_{vv}(\theta)$ practically shows no angular dependence and their $\langle R_g \rangle$ values cannot be accurately determined. Fig. 3 shows a typical measured intensity-intensity time correlation function for 6FDA-PFMB in THF at $\theta = 30°$ and $T = 30\,^{\circ}C$. It is known that for a polydisperse sample $g^{(1)}(t, q)$ is related to the line-width distribution ($G(\Gamma)$ by[10]

$$g^{(1)}(t,q) = \langle E(t,q)E^*(0,q)\rangle = \int_0^\infty G(\Gamma)e^{-\Gamma t}d\Gamma \tag{3}$$

Tab. 1. Summary of static and dynamic laser light-scattering results of five 6FDA-PFMB fractions

Sample	$10^{-4} \cdot \bar{M}_w$ g/mol	$\langle R_g \rangle$ nm	$10^4 \cdot A_2$ mol · cm^3 · g^{-2}	$10^8 \cdot \langle D \rangle$ cm^2 · s^{-1}	k_d mL · g^{-1}	f	$\langle R_h \rangle$ nm	$\langle R_g \rangle / \langle R_h \rangle$	$10^{-4} \cdot (\bar{M}_w)_{calcd}$ g · mol^{-1}	$\bar{M}_z/\bar{M}_w$	$\bar{M}_w/\bar{M}_n$
6FDA-1	20.3	41.9	10.3	22.4	75	~1	22.6	1.85	20.0	2.2	1.9
6FDA-2	13.4	32.4	11.2	28.1	41	~1	18.0	1.80	13.9	1.9	1.7
6FDA-3	5.99	17.4	28.2	48.2	27	~0	10.5	1.66	5.37	1.8	1.6
6FDA-4	1.54	–	23.0	94.8	13	~0	5.35	–	1.64	1.7	1.6
6FDA-5	0.69	–	53.4	149	~0	~0	3.38	–	0.68	2.4	2.0

The relative errors: $\bar{M}_w$, ±5%; $\langle R_g \rangle$, ±10%; A_2, ±15%; $\langle D \rangle$, ±1%.

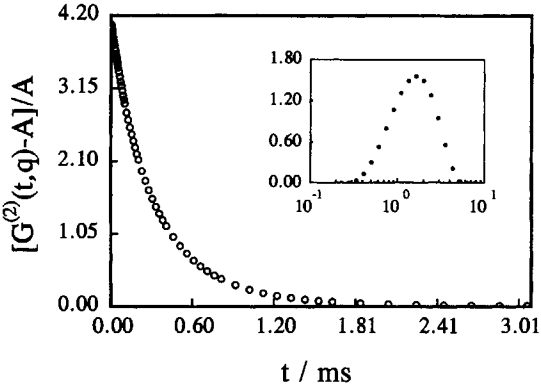

Fig. 3. Typical measured intensity-intensity time correlation function for 6FDA-PFMB in THF at $\theta = 30°$ and $T = 30$ °C. The insert shows a corresponding line-width distribution calculated from $G^{(2)}(t, q)$

The Laplace inversion program CONTIN was used in this work to convert $G^{(2)}(t, q)$ to $(G(\Gamma)$ on the basis of Eqs. 2 and 3. The insert in Fig. 3 shows such a $(G(\Gamma)$. The line width Γ usually depends on both C and q as[13, 14],

$$\Gamma/q^2 = D(1 + k_d C)(1 + f\langle R_g^2\rangle_z q^2) \tag{4}$$

where D is the z-averaged translational diffusion coefficient at $C \to 0$, and $q \to 0$; k_d, the diffusion second virial coefficient; and f, a dimensionless parameter depending on the chain structure, polydispersity, and solvent quality. k_d reflects both the thermodynamic and hydrodynamic interactions, i.e., $k_D = 2A_2\overline{M}_w - C_D N_A R_h^3/\overline{M}_w$, where C_D is a constant and R_h is the hydrodynamic radius. In general, f decreases as $\overline{M}_w$ increases and is in the range of 0.1 ~ 0.33. The values of $\langle D\rangle$, f, and k_d respectively from $(\Gamma/q^2)_{c\to 0,\theta\to 0}$, $(\Gamma/q^2)_{c\to 0}$ versus q^2 and $(\Gamma/q^2)_{\theta\to 0}$ versus C are also listed in Tab. 1. The values of f (~0.1) agree well with that predicted for a flexible polymer chain in a good solvent. In a good solvent ($A_2 > 0$), Γ/q^2 is less dependent on C than $R_{vv}(\theta)$ because of a partial cancellation of the hydrodynamic interaction ($C_D N_A R_h^3/\overline{M}_w$). In this study, $C \sim 10^{-4}$ and $\theta < 30°$ so that $(1 + k_d C)(1 + f\langle R_g^2\rangle_z q^2) \sim 1$ and $\Gamma/q^2 \approx D$. $G(\Gamma)$ can be transformed into a translational diffusion coefficient distribution $G(D)$ or a hydrodynamic radius distribution $f(R_h)$ using the Stokes-Einstein equation: $D \equiv k_B T/(6\pi\eta R_h)$, where k_B, T, and η are the Boltzmann constant, the absolute temperature, and solvent viscosity, respectively.

Fig. 4 shows the translational diffusion coefficient distributions $G(D)$ of five 6FDA-PFMB fractions in THF at $T = 30$ °C. From each $G(D)$, we were able to calculate a z-average translational diffusion coefficient $\langle D\rangle$ [$\equiv \int_0^\infty G(D)D\,dD$] and an average hydrodynamic radius $\langle R_h\rangle$ after replacing D in the Stokes-Einstein equation with $\langle D\rangle$. The values of $\langle D\rangle$, $\langle R_h\rangle$, and $\langle R_g\rangle/\langle R_h\rangle$ of five 6FDA-PFMB fractions are also summarized in Tab. 1. The ratios of $\langle R_g\rangle/\langle R_h\rangle$ are in the range of ~1.66–1.85 which agree well with the range (1.5–1.8) predicted for flexible polymer chains with a polydispersity index of $\overline{M}_w/\overline{M}_n \leq 2$ in a good solvent[15].

Fig. 5 shows $\log(\langle D\rangle)$ is a linear function of $\log_{10}(\overline{M}_w)$. The solid line represents a least-square fitting of $\langle D\rangle = \langle k_D\rangle \overline{M}_w^{-\langle a_D\rangle}$ with $\langle k_D\rangle = 2.13 \times 10^{-4}$ and $\langle a_D\rangle = 0.560$, where $\langle\ \rangle$ means that the values of $\langle k_D\rangle$ and $\langle a_D\rangle$ were obtained from $\langle D\rangle$ and $\overline{M}_w$

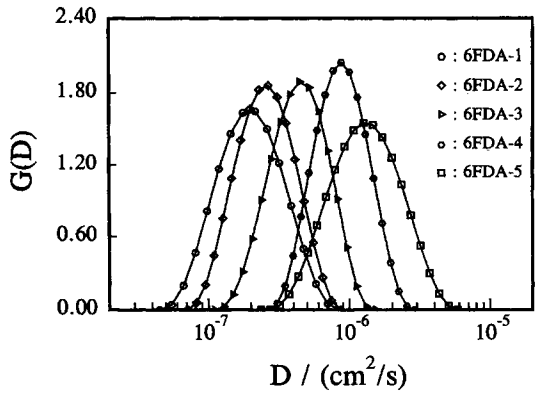

Fig. 4. Translational diffusion coefficient distributions, $G(D)$, of five 6FDA-PFMB fractions in THF at $T = 30\,^{\circ}C$

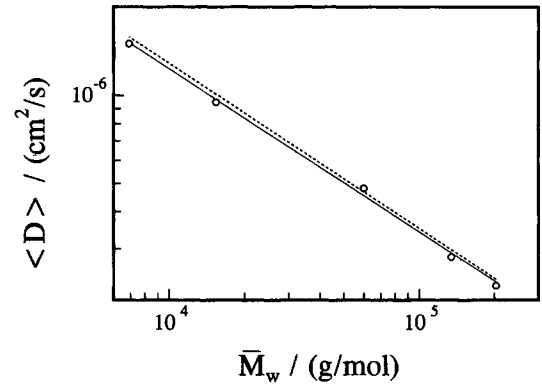

Fig. 5. Double logarithmic plot of $\langle D \rangle$ vs. $\bar{M}_w$, where the solid line represents the least-square fitting of $\langle D \rangle$ (cm^2/s) = $2.13 \times 10^{-4} \bar{M}_w^{-0.560}$ and the dotted line, D (cm^2/s) = $2.41 \times 10^{-4} M^{-0.564}$, where D and M correspond to monodisperse species

rather than from D and M for monodisperse species. The value of $\langle a_D \rangle = 0.560$ indicates that the 6FDA-PFMB chains have a coil conformation in THF at $T = 30\,^{\circ}C$. Using $\langle k_D \rangle$ and $\langle a_D \rangle$, we can transfer each $G(D)$ into a molecular weight distribution (MWD). The principle is as follows. On the one hand, in static LLS, when $C \rightarrow 0$ and $q \rightarrow 0$,

$$\int_0^\infty f_w(M)\, M\, dM \propto R_{vv}(q) \propto \langle I \rangle \tag{5}$$

where $f_w(M)$ is a weight-average molecular weight distribution. On the other hand, in dynamic LLS, as $t \rightarrow 0$,

$$[g^{(1)}(t,q)]_{t\rightarrow 0} = \int_0^\infty G(\Gamma)\, d\Gamma \propto \int_0^\infty G(D)\, dD \propto \langle I \rangle \tag{6}$$

A comparison of Eqs. 5 and 6 leads to

$$\int_0^\infty f_w(M)\, M\, dM \propto \int_0^\infty G(D)\, dD \tag{7}$$

or rewritten as

$$\int_0^\infty f_w(M)\, M^2\, d(\ln M) \propto \int_0^\infty G(D)\, D\, d(\ln D) \tag{8}$$

where $d(\ln M) \propto d(\ln D)$ since $D = k_D M^{-a_D}$. Eq. 8 leads to

$$f_w(M) \propto \frac{G(D)D}{M^2} \propto G(D) D^{1+2/a_D} \tag{9}$$

All proportionality constants have been omitted in Eqs. 5–9 since they are irrelevant to a given distribution. Using the definition of $\overline{M}_w [= \int_0^\infty f_w(M)\, M\, dM / \int_0^\infty f_w(M)\, dM]$ and Eq. 9, we have

$$(\overline{M}_w)_{calcd.} = \frac{k_D^{1/a_D} \int_0^\infty G(D)\, dD}{\int_0^\infty G(D)\, D^{1/a_D}\, dD} \tag{10}$$

Importing the values of $\langle k_D \rangle$ and $\langle a_D \rangle$ in Eq. 10, we found that the calculated values of $\overline{M}_w$ of 6FDA-1, 6FDA-2, 6FDA-3, 6FDA-4 and 6FDA-5 are 1.75×10^5, 1.22×10^5, 4.67×10^4, 1.41×10^4 and 5.85×10^3, respectively, which are smaller than the values of $\overline{M}_w$ measured directly from static LLS (listed in Tab. 1). This disagreement is because the 6FDA-PFMB fractions still have a moderate molecular weight distribution.

From our previous studies[16–18], a method of combining static and dynamic LLS results to obtain k_D and a_D from the measured values of $\overline{M}_w$ and $G(D)$ has been developed. The detail of this method can be found in refs.[16–18]. Using this method, we found that $a_D = 0.564$ and $k_D = 2.41 \times 10^{-4}$. This pair of k_D and a_D defines a relation between D and M for monodisperse 6FDA-PFMB in THF at $T = 30\,^\circ C$, as shown in Fig. 5 by the dotted line. With this pair of k_D and a_D, we are ready to convert each $G(D)$ in Fig. 4 to its corresponding $f_w(M)$.

Fig. 6 shows differential weight distributions $f_w(M)$ of five 6FDA-PFMB fractions. From each $f_w(M)$, we calculated a corresponding weight-average molecular weight $(\overline{M}_w)_{calcd}$ and polydispersity index $\overline{M}_w/\overline{M}_n$ and $\overline{M}_z/\overline{M}_w$ listed in Tab. 1. The values of $(\overline{M}_w)_{calcd}$ agree well with the values of $\overline{M}_w$ measured in static LLS. The values of $\overline{M}_w/\overline{M}_n \leq 2$ are expected since 6FDA-PFMB was made in a polycondensation.

We can estimate the persistence length (ℓ) on the basis of Benoit-Doty approach[19] namely $\langle R_g^2 \rangle = \ell^2\{1/3(L/\ell) - 1 + (2\ell/L) - (2\ell^2/L^2)[1 - \exp(-L/\ell)]\}$, where L (= $n\ell_u$) is the contour length with ℓ_u being the projected length of the monomer unit and n (= $\overline{M}_w/\overline{M}_0$) being the average number of monomer units on each chain. In this case, ℓ_u and $\overline{M}_0$ are ~2.2 nm and 728 g/mol, respectively. Strictly speaking, we should use n = $(\overline{M}_z/\overline{M}_w)(\overline{M}_w/\overline{M}_0)$ since $\langle R_g \rangle$ measured in static LLS is a z-averaged parameter. The value of ℓ estimated from five polyimide samples is ~3.3 nm which leads to the Flory characteristic ratio $C_\infty \sim 40$ on the basis of $C_\infty = (2\ell/l_0) - 1$[20]. In comparison, for typical flexible polymers, such as polystyrene and poly(methyl methacrylate), in good solvent, $\ell \sim 1$ nm and $C_\infty \sim 10$. Therefore, the 6FDA-PFMB chain is much extended in THF at 30 °C.

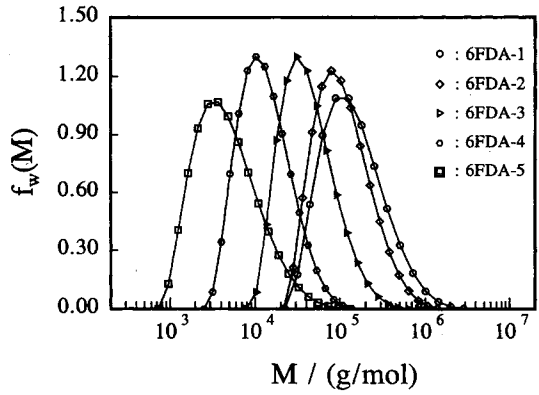

Fig. 6. Differential weight distributions of five 6FDA-PFMB fractions

Fig. 7 shows a double logarithmic plot of $\langle R_h \rangle$ vs $\bar{M}_w$. The solid line represents a least-square fitting of $\langle R_h \rangle$ (nm) = 2.38 × 10^{-3} $\bar{M}_w^{0.560}$. The exponent values (~0.56) further implies that the 6FDA-PFMB chains have a coil chain conformation in THF at 30 °C. Moreover, for comparison, we also plot "$\langle R_h \rangle$ versus $\bar{M}_w$" for polystyrene in toluene in Fig. 7 (the dashed lines)[21]. It can be seen that the solid lines have a similar slope as the dashed lines, which indicates that the 6FDA-PFMB chain in THF as polystyrene has a random-coil conformation, which can be attributed to the hexafluoroisopropylidene group between the aromatic rings.

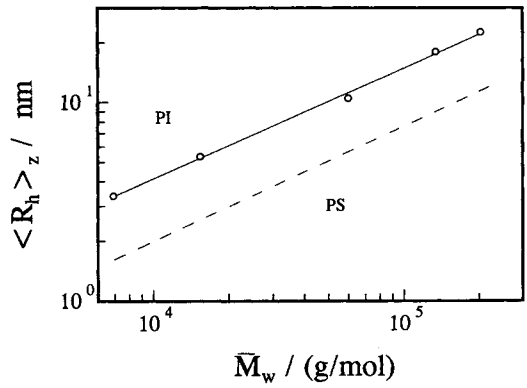

Fig. 7. Plot of $\log_{10}(\langle R_h \rangle)$ vs. $\log_{10}(M_w)$, where solid line represents the least-square fitting of $\langle R_h \rangle$ (nm) = 2.38 × 10^{-3} $\bar{M}_w^{0.560}$ for 6FDA-PFMB in THF; and the dashed line, $\langle R_h \rangle$ (nm) = 9.99 × 10^{-3} $\bar{M}_w^{0.577}$ for polystyrene in toluene

Conclusion

A combination of static and dynamic laser light scattering studies of 6FDA-PFMB in THF at 30 °C has shown that (i) THF is a thermodynamically good solvent for 6FDA-PFMB at 30 °C; (ii) the persistence length (ℓ) of 6FDA-PFMB and Flory characteristic ratio C_∞ are ~3.3 nm and ~40, respectively, which reveals that the 6FDA-PFMB chain is more extented than typical random-coil chains; (iii) the values of $\langle R_g \rangle / \langle R_h \rangle$ are in the range of 1.66–1.85; and (iv) the following relations: A_2 (mol · cm^{-3} · g^{-2}) = 2.1 × 10^{-1} $\bar{M}_w^{-0.43}$ and D (cm^2/s) = 2.41 × 10^{-4} × $M^{-0.564}$ have been established. Using the relation between D and M, we have successfully con-

verted each translational diffusion coefficient distribution into a corresponding differential weight distribution. These relations will enable us to characterize 6FDA-PFMB with only one concentration and one scattering angle in future. In comparison with polystyrene, we conclude that the 6FDA-PFMB chain has an extended coil conformation in THF at 30 °C on the basis of the values of $\langle R_g \rangle / \langle R_h \rangle$, ν, C_∞, and the exponents of the relations.

Acknowledgment: The financial support of this work by *RGC (the Research Grants Council of Hong Kong Government) Earmarked Grants* 1995/96, (CUHK 299/94P, A/C No. 221600260) is gratefully acknowledged.

[1] D. Wilson, H. D. Stengenberger, P. M. Hergenrother, *Polyimides*; Chapman and Hall, New York 1990
[2] T. Matsuura, Y. Hasuda, S. Nishi, N. Yamada, *Macromolecules* **24**, 5001 (1991)
[3] S. Kim, P. M. Cotts, W. Volksen, *J. Polym. Sci., Part B.* **30**, 177 (1992)
[4] S. A. Swanson, R. Siemens, P. Cotts, *Polyimides: Materials, Chemistry and Characterization*, C. Feger, Ed., Elsevier Science, New York 1989
[5] A. E. Feiring, B. C. Auman, E. R. Wonchoba, *Macromolecules* **26**, 2779 (1993)
[6] T. Matsuura, M. Ishizawa, Y. Hasuda, S. Nishi, *Macromolecules* **25**, 3540 (1992)
[7] S. L.-C. Hsu, Ph.D Dissertation, Department of Polymer Science, The University of Akron, Akron, Ohio, 44325-3909, 1991
[8] S. Lin, Ph.D Dissertation, Department of Polymer Science, The University of Akron, Akron, Ohio, 44325-3909, 1994
[9] R. Pecora, J. Berne, *Dynamic Light Scattering,* Plenum Press, New York 1976
[10] B. Chu, *Laser Light Scattering, 2nd ed.,* Academic Press, New York 1991
[11] B. H. Zimm, *J. Chem. Phys.* **16**, 1099 (1948)
[12] C. Wu, K. Q. Xia, *Rev. Sci. instrum.* **65** (3), 587 (1994)
[13] W. H. Stockmayer, M. Schmidt, *Pure Appl. Chem.* **54**, 407 (1982)
[14] W. H. Stockmayer, M. Schmidt, *Macromolecules 17*, 509 (1984)
[15] W. Burchard, M. Schmidt, W. H. Stockmayer, *Macromolecules* **13**, 1265 (1980)
[16] C. Wu, *Colloid Polym. Sci.* **271**, 947 (1993)
[17] C. Wu, *J. Polym. Sci., Polym. Phys.* **32,** 803 (1994)
[18] C. Wu, J. Zuo, B. Chu, *Macromolecules* **22,** 633 (1989)
[19] H. Benoit, P. Doty, *J. Phys. Chem.* **57**, 958 (1953)
[20] Z. Xu, N. Hadjichristidis, L. J. Fetters, J. W. Mays, *Adv. Polym. Sci.* **120**, 1 (1995)
[21] B. Appelt, G. Meyerhoff, *Macromolecules* **13**, 657 (1980)